

Role of chemical potential in relaxation of faceted crystal structure

Joshua P. Schneider¹, Kanna Nakamura¹, and Dionisios Margetis^{1,2}

¹*Department of Mathematics, University of Maryland, College Park, Maryland 20742, USA*

²*Institute for Physical Science and Technology, and Center for Scientific Computation and Mathematical Modeling, University of Maryland, College Park, Maryland 20742, USA*

(Dated: April 25, 2014)

Below the roughening transition, crystal surfaces have macroscopic plateaus, facets, whose evolution is driven by the microscale dynamics of steps. A long-standing puzzle was how to reconcile discrete effects in facet motion with fully continuum approaches. We propose a resolution of this issue via connecting, through a *jump condition*, the continuum-scale surface chemical potential away from the facet, characterized by variations of the continuum surface free energy, with a chemical potential originating from the decay of atomic steps on top of the facet. The proposed condition accounts for step flow inside a *discrete boundary layer* near the facet. To validate this approach, we implement in a radial geometry a hybrid discrete-continuum scheme in which the continuum theory is coupled with *only a few, minimally three*, steps in diffusion-limited kinetics with conical initial data.

PACS number(s): 68.35.Md, 68.43.Jk, 61.50.Ah

I. INTRODUCTION

Material systems can in principle be described by equations governing the motion of their discrete constituents. This approach requires resolving many degrees of freedom. If variables of interest exhibit smooth behavior at macroscopic scales, an alternative is to apply continuum models, e.g., partial differential equations (PDEs), that result from appropriately averaging out microscopic details. Continuum equations are appealing since they are amenable to analytical predictions such as scaling laws testable in lab experiments. Moreover, continuum descriptions offer computational advantages over discrete schemes for large-scale simulations. Many macroscopic systems, however, have small spatial regions where dependent variables of interest exhibit *singular* behavior; examples of such regions are edges of macroscale plateaus (facets) on crystal surfaces, tips of cracks in brittle solids, and contact lines of liquid films. These small regions may dramatically influence evolution at macroscopic length and time scales. A classic question is: How can such microscale effects be incorporated into continuum theories?

In this paper, we propose a scenario for incorporating the edges of facets into a continuum thermodynamics framework consistent with the discrete flow. At the microscale, crystal surface evolution is driven by the motion of many atomic line defects, steps. At the macroscale, a PDE for the surface height outside the facet offers a plausible description; physically relevant solutions to this PDE have singular behavior near the facet edge. We reconcile these two scales by imposing a *step-driven discontinuity* of the surface chemical potential across the facet edge, modifying the previously applied notion of a continuous chemical potential. To illustrate our approach with relative computational ease, we focus on an idealized model: a semi-infinite axisymmetric structure with a single facet in the absence of material deposition from above. We study long-time surface relaxation, when the slope profile exhibits self similarity.

Our main contributions with this work are:

(a) We *empirically* construct a global, macroscopic surface chemical potential, μ_S , that expresses: (i) changes of the continuum-scale free energy of many steps away from the facet; and (ii) the annihilation of individual atomic steps on the facet. These two distinct physical characterizations of μ_S must suitably be *connected* across the facet edge. To this end, we propose a jump condition that accounts for details inside a narrow region of a few steps, herein called a *discrete boundary layer*, near the facet.

(b) We formulate a continuum theory outside the facet that implicitly accounts for the discrete boundary layer. The resulting *free boundary problem* for the facet consists of: (i) a continuum equation for the self-similar surface slope away from the facet; and (ii) boundary conditions by which the large-scale surface chemical potential and a flux generating it are forced to have jump discontinuities at the facet edge as described in (a).

(c) To validate our approach, we formulate and implement a computational scheme, henceforth referred to as the “hybrid scheme”, to approximately solve the above free boundary problem without resolving the full step system. As the time, t , advances, our scheme successively improves the slope profile through the solution of discrete equations for a few, minimally three, steps inside the boundary layer. We show by numerics that our scheme apparently converges to the surface slope profile computed via independent many-step simulations.

From a physical perspective, our approach exemplifies the key role of the surface chemical potential, μ_S , in reconciling two seemingly disparate notions: (i) the facet, a macroscopic object; and (ii) the (discrete) step. Our work indicates that the facet and the bulk of steps away from it can be treated as two distinct “phases” connected through an unusual jump condition for μ_S . The magnitude of this jump depends on the continuum surface profile *and* the curvatures of individual steps in the discrete boundary layer; this layer represents the microstructure of the interface between the two phases.

There is a long sequence of works analyzing facet mo-

tion under diffusion of adsorbed atoms (adatoms). A difficulty in the application of continuum theories stems from microscale effects, namely, the collapses of atomic steps on top of facets [1–4]. A central question is how to incorporate such collapses into the continuum setting.

A plausible continuum approach, pioneered in [5], is to treat the facet edge as a free boundary: apply a PDE, which is herein viewed as the continuum limit of step flow, for the surface height or slope on the smooth surface region, outside the facet, and supply appropriate boundary conditions at the facet edge. The choice of boundary conditions is crucial. In the case of surface diffusion without external material deposition, crystal structures usually relax to become flat by lowering the total surface free energy. In this context, boundary conditions at the facet edge may result from thermodynamic arguments, particularly the assumption that every point on the surface evolves by causing the most rapid decrease to the continuum-scale surface free energy [6]. It turns out that, as a consequence of this ansatz, the continuum surface height, positive slope and adatom flux normal to the facet boundary are continuous; in addition, the chemical potential, defined as the change per atom of the surface free energy, is extended continuously onto the facet [5, 7]. Nonetheless, the imposition of the above conditions, which we will refer to as the “reference case”, has been shown to be *inconsistent* with step motion [8, 9]. Works that invoke a modified, smoothed surface free energy or truncated Fourier expansions for the surface height have the same flavor [10–12].

A means of reconciling step motion with continuum theory near facets is offered by asymptotic matching of the surface slope profile across the facet edge via appropriate series expansions [3, 4, 13, 14]. In settings where atomic steps collapse on top of the facet, this view requires discrete details, i.e., the times of step collapses [3, 4]; such details become available through solving a large system of differential equations for step positions.

An emerging question is: Can a reliable model of facet evolution be constructed by coupling the continuum theory outside the facet with the motion of *only a few* steps near the facet? Such a model would be an appealing alternative to the use of the whole set of discrete step equations: First, it would be amenable to scaling predictions, possibly testable in lab experiments; and, second, the model would reduce the computational complexity of integrating a large number of discrete equations.

Here, we aim to provide an answer to the above question. Our idea is to introduce a surface chemical potential that is *discontinuous* across the facet edge. The magnitude of the discontinuity is controlled both by the global surface profile and the discrete dynamics of a few special steps near the facet. This idea has the potential of application to arbitrary geometries with facets.

This perspective, especially the use of discontinuities for thermodynamic variables at the facet edge, has been inspired by a recent analysis of an evaporation-

condensation dynamics model [15]. In [15], the jump is introduced only for the radial flux generating the continuum-scale chemical potential. Here, we need additional boundary conditions (since the PDE is of higher order) [16–18]. In fact, we impose jumps for *both* the large-scale chemical potential and its generating flux in terms of a discrete geometric factor. Our definitions of jump discontinuities are primarily phenomenological.

In order to computationally validate our approach, we apply a hybrid scheme. This scheme resolves simultaneously the fast motion of a few top steps, near the facet, and the relatively slow surface relaxation away from the facet. The underlying two-scale strategy offers some insight into the nature of continuum solutions near the facet; in particular, the singularity for the surface slope at the facet edge emerges as a pathology of the continuum limit because of the reduction of the discrete boundary layer to the sharp facet boundary.

It is of some interest to compare our approach to previous continuum models where atomic steps are annihilated on top of facets, e.g., [3–5, 7–9, 15]. For example, in [5, 7] only the continuity of the surface chemical potential, which yields results not consistent with step flow, is considered. In [3, 4, 9, 15] the *entire* many-step system is simulated for reconciling continuum predictions with step motion. In [8], a continuum-type equation is formulated from an ensemble of step configurations, and the facet boundary is not treated explicitly.

Alternate boundary conditions at the facet edge have been invoked. In [3, 4], the continuity of the macroscopic chemical potential is replaced by the statement that the vertical facet speed must follow discrete changes of the facet height, called the “step-drop condition”. This latter condition requires the use of the differences, δt_n , of step collapse times, and involves high spatial derivatives of the surface height at the facet edge. Thus far, the step-drop condition is not deemed appealing for coupling steps with continuum solutions for at least two reasons. First, from a physical perspective, the step-drop condition appears unnatural within the continuum thermodynamics framework. Second, the resulting slope profiles are too sensitive to any errors in δt_n ; hence, the convergence of any associated scheme is too difficult to achieve numerically. Here, we keep variables of the continuum framework but make an attempt to reconcile them with the (non-equilibrium) discrete scheme for steps.

It is worthwhile noting that our approach has the flavor of multiscale methods in mechanics and applied mathematics; see, e.g. [19–22]. In particular, the quasicontinuum method [19] addresses the coupling of macroscopic equations to the atomistic structure. Key aspects of our treatment are tailored to the physics of the facet. Hence, direct comparisons of our approach to existing multiscale methods lie beyond our present scope.

We describe discrete step flow via the classic models by Kossel [23], Stranski [24], and Burton, Cabrera and Frank [25]; for reviews on later additions to these models, see [26, 27]. Each step interacts with its nearest neigh-

bors through force-dipole and entropic repulsion [28, 29]. At this microscale level, adatoms diffuse on nanoscale terraces and attach to or detach from steps; as a result, steps move by mass conservation. We assume that adatom diffusion is the slowest process, restricting attention to the “diffusion-limited kinetics” regime. Hence, there are two main ingredients of step motion, namely, step *energetics*, expressed via near-equilibrium thermodynamic concepts such as the step chemical potential; and diffusion-limited *kinetics*, reflected in the relation of adatom flux and step chemical potential. These ingredients form our step flow model. For comparison purposes, we numerically solve the resulting large system of ordinary differential equations (ODEs) for the step radii by imposing initial data for a linear cone. At sufficiently long time, the terrace width or discrete slope (inverse of terrace width) exhibits the anticipated self-similar behavior [3, 4].

In the continuum limit away from the facet, step energetics give rise to a surface free energy whose variational derivative produces the large-scale chemical potential, μ , the continuum limit of the step chemical potential. At this level of description, the physical facet mathematically corresponds to a particular type of singularity of the free energy density, as a function of surface orientation, at vanishing surface slope. We believe that our scheme implicitly smooths out the surface free energy by taking into account the motion of steps inside the discrete boundary layer. We are aware that this approach in principle implies a modified surface free energy close to the facet. By treating the facet edge as a moving boundary, we circumvent the use of such an energy.

Our approach has limitations. The analytic *derivation* of facet boundary conditions from step flow remains an open problem. Because of our self-similarity ansatz at the continuum scale, we do not describe transient dynamics, for which the full evolution PDE away from the facet is needed. The convergence of our hybrid scheme is not studied. Kinetic regimes other than diffusion-limited kinetics are not addressed. We consider only initial conical data. The extension of our approach to two spatial dimensions (2D) is not developed.

The remainder of the paper is organized as follows. Section II provides an overview of the step flow model and corresponding continuum theory. In Sec. III, we formulate the step ODEs and describe (i) the free boundary problem of the reference case, and (ii) the modified free boundary problem in terms of jump discontinuities depending on the positions of steps inside the discrete boundary layer. In Sec. IV, we describe our hybrid scheme. Section V presents some numerical results. In Sec. VI, we discuss plausible modifications of our work. Finally, in Sec. VII we summarize our results.

II. BACKGROUND

In this section, we briefly review basic elements of the step flow model [23–25] and the respective continuum de-

scription. We emphasize the special character of faceted surface regions in the continuum framework.

A. Step flow model: A review

Steps are represented by smooth curves separated by terraces and move as adatoms attach to or detach from step edges. Adatoms can diffuse across terraces. We neglect step edge diffusion and evaporation of adatoms, and assume that no material is deposited on the surface from above. The concentration $C(\mathbf{r}, t)$ of adatoms on terraces obeys

$$\frac{\partial C}{\partial t} = \nabla \cdot (D_s \nabla C), \quad (1)$$

where D_s is the (constant for our purposes) terrace diffusivity. In the *quasistatic regime*, we set $\partial C / \partial t \approx 0$ [30]. The validity of this approximation for fast-moving top steps is an open issue not addressed here.

At each step we impose the kinetic relation [31]

$$J_{\pm, \perp} = k_{\pm}(C_{\pm} - C^{\text{eq}}); \quad (2)$$

see also [25] for the special case $C_{\pm} = C^{\text{eq}}$ and related reviews in [26, 27]. Here, $J_{\pm, \perp}$ is the restriction at the step edge of the component of the adatom flux $\mathbf{J}_{\pm} = -D_s \nabla C$ on the upper (+) or lower (−) terrace normal to and directed toward the step; k_{\pm} is the respective rate of attachment-detachment due to the Ehrlich-Schwoebel barrier [32]; C_{\pm} is the value of the adatom concentration at the step on the corresponding terrace; and C^{eq} is the local equilibrium concentration at the step edge. For diffusion-limited kinetics, the diffusion length D_s/k_{\pm} is considered small compared to the typical terrace width.

Equations (1) and (2) are linked to step energetics via

$$C^{\text{eq}} = c_s \exp\left(\frac{\mu_{\text{st}}}{k_B T}\right) \approx c_s \left(1 + \frac{\mu_{\text{st}}}{k_B T}\right), \quad (3)$$

where μ_{st} is the step chemical potential, c_s is a constant concentration, and $k_B T$ is the Boltzmann energy [33]; $|\mu_{\text{st}}| \ll k_B T$. In particular, μ_{st} is the change in the step free energy by addition of an atom to the step. It was recently shown that if U_{st} is the step free energy per unit length, μ_{st} is given by [34]

$$\mu_{\text{st}} = \frac{\Omega}{a} \nabla \cdot (U_{\text{st}} \mathbf{e}_{\eta}), \quad \eta = \eta_{\text{st}}, \quad (4)$$

and thus depends on the step configuration via U_{st} . Here, Ω is the atomic volume, a is the step height, and the step edge curve is described by $\eta = \eta_{\text{st}}$ in a curvilinear coordinate system, (η, ς) , with unit normal vector \mathbf{e}_{η} ; $U_{\text{st}} = U(\eta, \varsigma)$. If $U = \beta$, Eq. (4) yields $\mu_{\text{st}} = (\Omega/a)\beta \kappa_{\text{st}}$ where κ_{st} is the local step edge curvature, as expected [33].

By mass conservation, the normal step velocity is [25]

$$v_{\text{st}} = \frac{\Omega}{a} (J_{+, \perp} + J_{-, \perp}). \quad (5)$$

Equations (1)–(5) describe step motion given initial data for step positions.

B. Continuum limit away from facet

Next, for a monotone step train and diffusion-limited kinetics, we outline elements of the continuum theory away from the facet, in correspondence to the step flow model of Sec. II A. In the continuum limit, $a/\lambda \rightarrow 0$ while the step density is kept fixed, where λ is a typical macroscopic length. Details on the formal *derivation* of the continuum limit in 2D can be found in [34].

First, the step velocity, v_{st} , approaches $(\partial h/\partial t)/|\nabla h|$. Accordingly, step motion law (5) becomes the mass conservation statement

$$\frac{\partial h}{\partial t} + \Omega \nabla \cdot \mathfrak{J} = 0, \quad (6)$$

where $\mathfrak{J}(\mathbf{r}, t)$ is the continuum-scale adatom flux.

Second, Eqs. (1)–(3) give rise to a constitutive relation between the large-scale adatom flux, $\mathfrak{J}(\mathbf{r}, t)$, and the macroscale chemical potential, $\mu(\mathbf{r}, t)$ [34]:

$$\mathfrak{J}(\mathbf{r}, t) = -\frac{c_s D_s}{k_B T} \mathbf{M} \cdot \nabla \mu, \quad (7)$$

where \mathbf{M} is an orientation-dependent (dimensionless) tensor. For diffusion-limited kinetics, where $[D_s/(ka)]|\nabla h| \ll 1$, this \mathbf{M} reduces to $\mathbf{1}$, the unit tensor [17].

Third, by Eq. (4) the continuum-scale chemical potential, μ , is the variational derivative of the surface free energy, $E[h]$, the continuum limit of aU_{st} [33]:

$$\mu = \Omega \frac{\delta E}{\delta h}, \quad (8)$$

provided the right-hand side is well defined. For entropic and force-dipole step-step interactions, the free energy, $E[h]$, of a vicinal surface reads [6]

$$E[h] = \iint \left(g_0 + g_1 |\nabla h| + \frac{1}{3} g_3 |\nabla h|^3 \right) dS, \quad (9)$$

where g_0 is the energy per area of the (x, y) -reference plane, $g_1 a = \beta$ is the step line tension, g_3 accounts for repulsive step-step interactions, $g_3 > 0$, and $dS = dx dy$. Notably, $\delta E[h]/\delta h$ is (locally) ill defined at surface regions where $\nabla h = 0$, which correspond to facets in this formulation (Sec. II C) [6]. By Eq. (8), the variable μ is

$$\mu = \Omega g_1 \nabla \cdot \boldsymbol{\xi}, \quad (10)$$

where

$$\boldsymbol{\xi} = -\left(1 + g|\nabla h|^2\right) \frac{\nabla h}{|\nabla h|}, \quad \mathbf{r} : \text{outside facet}, \quad (11)$$

and $g = g_3/g_1$ expresses the relative strength of step-step interactions and step line tension.

The combination of Eqs. (6), (7) and (10) for diffusion-limited kinetics yields a fourth-order PDE for h :

$$\frac{1}{B} \frac{\partial h}{\partial t} = \nabla^2 (\nabla \cdot \boldsymbol{\xi}), \quad (12)$$

which is valid outside facets; $\boldsymbol{\xi}$ is defined by Eq. (11) and $B = c_s D_s \Omega^2 g_1 / (k_B T)$ is a material parameter [17].

C. Facet as special free boundary

We now discuss aspects of the free boundary view for the evolution of a faceted structure. As is indicated in Sec. II B, PDE (12) with Eq. (11) is questionable at the facet, where $\nabla h = 0$ according to Eq. (9). In the mathematics literature, a remedy to this pathology has been offered by a formalism (“subgradient formalism”) that treats the facet as part of the PDE solution [35, 36]. This approach is consistent with the smoothing of the energy $E[h]$ in [10]; the treatment of the facet by use of an analogy with porous-media equations in [5]; and the application of (truncated) Fourier series expansions for the surface height in [12]. In this context, the continuum is self-contained. In the spirit of [35], PDE (12) is applied *everywhere* on the surface; then, $\boldsymbol{\xi}$ must appropriately be extended from the smooth sloping surface onto the facet. A mathematically plausible extension follows from the property that relaxation occurs as the steepest descent, in some appropriate metric, of the surface free energy, $E[h]$. This approach implies a certain free boundary problem [5]: Apply PDE (12) away from the facet and enforce boundary conditions at the facet edge that include the continuous extensions of the continuum-scale (i) surface height, (ii) positive surface slope, $|\nabla h|$, (iii) adatom flux normal to the facet edge, and (iv) chemical potential, μ . The component of $\boldsymbol{\xi}$ normal to the facet edge is also continuously extended onto the facet. In addition, far-field conditions on a semi-infinite structure require that the height and positive slope approach their initial data far from the facet. This set of conditions forms our reference case, to be used for comparisons to an alternate continuum theory (Sec. III E).

The above treatment of the facet is dictated by fully continuum considerations. An emerging issue has been whether the resulting macroscopic evolution is consistent with the dynamics of step flow.

It has been demonstrated by simulations for a faceted axisymmetric crystal structure under diffusion-limited kinetics that the continuum slope determined in the reference case is not consistent with step motion [8]. For an analogous result in evaporation-condensation kinetics, see [15]. In fact, it has been realized that the facet is a special region where discrete effects, especially collapses of steps, may dramatically influence the large-scale surface morphology [4].

In [9], predictions of the continuum model are reconciled with step flow simulations by replacement of the continuity of the continuum-scale chemical potential by a drastically different condition, the step-drop condition, inspired by [4]. This latter condition requires that, in settings where the facet is a plateau of zero surface slope, the facet height, $h_f(t)$, decrease by increments of a single atomic height at each step collapse:

$$h_f(t_{n+1}) - h_f(t_n) = -a, \quad (13)$$

where t_n is the n th-step collapse time. Equation (13) can be viewed as a condition on the discrete derivative

of $h_f(t)$, where $t \approx t_n$, and is approximately reduced to

$$\dot{h}_f \approx -\frac{a}{\delta t(t)}, \quad \delta t(t) = t_{n+1} - t_n, \quad (14)$$

which imposes a vertical facet speed given the time difference $\delta t(t)$ [9]. Note that the dot on top of a symbol denotes differentiation with respect to time.

Because each t_n is in principle computed by solving all step flow equations, Eq. (14) reveals the nonlocal coupling of facet motion with the surface profile through step flow. The quantity $\delta t(t)$ depends on the dynamics of the many-step system. Equation (14) leads to predictions consistent with steps [9]; however, it is deemed as impractical for computing large-scale surface morphologies: First, the accurate evaluation of $\delta t(t)$ may require simulations of a large number of steps. Second, Eq. (14) leads to a boundary condition sensitive to errors in $\delta t(t)$.

An alternate scenario avoiding Eq. (13) was proposed in [15] for an evaporation-condensation model in a radial geometry. In this case, the evolution PDE takes the form $\partial h / \partial t = -\nu \Omega g_1 \text{div} \boldsymbol{\xi}$ everywhere [cf. Eq. (12)], where ν is a material parameter. Then, the boundary conditions serving as the reference case consist of continuity of: height, radial flux variable $\boldsymbol{\xi}$, and slope if $g_3 > 0$ [cf. Eqs. (10) and (11)]. The resulting free boundary problem in principle yields predictions not consistent with step flow [15]. Instead of the use of the step-drop condition as a remedy, in [15] the radial $\boldsymbol{\xi}$ is required to have a jump discontinuity at the facet edge [15]. The continuity of height and slope are left intact. Specifically, in axisymmetry, if $\xi_f(r, t)$ is the radial component of $\boldsymbol{\xi}$ on the facet, r is the polar coordinate, and $r_f(t)$ is the facet radius, the jump condition reads

$$\xi_f(r, t) \Big|_{r_f(t)^-} = Q(t) \xi_f(r, t) \Big|_{r_f(t)^+}, \quad (15)$$

where r_f^\pm indicates the limit as r approaches the facet edge from outside (+) or inside (-) the facet. Here, $Q(t)$ represents a piecewise-constant multiplicative jump depending on the radii of two top steps at collapse times through the geometric factor $[r_{n+1}(t_{n-1}) + r_n(t_{n-1})] / [2r_{n+1}(t_{n-1})]$ for $t_{n-1} \leq t < t_n$ ($n \geq 1$); $r_i(t)$ is the i -th step radius. For large enough time, step simulations reveal that $Q(t) \approx 3/4$ [15]. The resulting continuum theory is found to be in excellent agreement with step flow simulations [15]. It has been argued that in this case *the facet moves vertically much in the same way that a shock wave propagates in a fluid* [15]; by mass conservation, the condition for the shock-wave speed entails Eq. (15) with the above value for Q [15].

Here, we make the attempt to extend some of these insights to the case with diffusion-limited kinetics. We consider jump discontinuities in *both* the global chemical potential and its generating flux, $\boldsymbol{\xi}$ (see Sec. III). From a physical viewpoint, this approach aims to reconcile the thermodynamic structure of macroscopic evolution laws, e.g., Eq. (8), with the microstructure of step flow near the facet via suitable factors that reveal details of the

discrete boundary layer. We view this approach as a potential guide to more systematic studies in 2D.

III. RADIAL GEOMETRY: FORMULATION AT TWO SCALES

In this section, we describe the radial geometry of the faceted crystal, provide the governing equations of motion for steps in diffusion-limited kinetics, and formulate two free boundary problems at the continuum scale. One of these formulations is the reference case. Another formulation uses jump boundary conditions for the large-scale chemical potential and its generating flux.

A. Geometry

At the macroscale, the axisymmetric crystal surface is represented by the height profile, $h(r, t)$ (see Fig. 1). The crystal structure is taken to be semi-infinite for our purposes. The facet, which is assumed to have fixed orientation of zero slope ($\partial h / \partial r = 0$), has height $h_f(t)$ and radius $r_f(t)$. It is expected that $h_f(t)$ is monotonically decreasing and $r_f(t)$ is increasing with t .

At the microscale, the crystal structure consists of a monotone step train with concentric circular steps of atomic height, a (Fig. 1). The i th-step radius is $r_i(t)$. Initially (at $t = 0$), there are N steps with radii $r_i(0)$, where $r_i(0) < r_{i+1}(0)$, $1 \leq i \leq N$ and $N \gg 1$ ($r_{N+1} = \infty$). The n th-step collapse time, t_n , is defined by $r_n(t) \equiv 0$ for $t \geq t_n$ and $r_n(t) > 0$ for $t < t_n$ ($1 \leq n \leq N$). For $t_n < t < t_{n+1}$, there are $N - n$ moving steps and the i th terrace is the region $r_i(t) < r < r_{i+1}(t)$, which has width $r_{i+1} - r_i$, $n \leq i \leq N - 1$; N approaches infinity for our purposes. We hypothesize that the initial ordering of steps is preserved by the flow for all times $t > 0$, since the force-dipole step repulsion prevents their crossing [cf. Eqs. (18) and (19) below]. The discrete slope is

$$m_i(t) = \frac{a}{r_{i+1}(t) - r_i(t)}, \quad (16)$$

assumed to be positive ($m_i(t) > 0$).

B. Microscale: Step motion laws

Next, we briefly describe the governing step equations. Some details can be found in [4, 7]. In the radial geometry, diffusion equation (1) in the quasi-static regime is solved exactly on each terrace with Eqs. (2) and (3) at the bounding step edges. By diffusion-limited kinetics, when $D_s / [k_\pm (r_{i+1} - r_i)] \ll 1$, the resulting adatom flux, $J_i(r, t)$, on the i th terrace is

$$J_i(r, t) = -\frac{D_s c_s}{k_B T} \frac{\mu_{i+1} - \mu_i}{\ln \frac{r_{i+1}}{r_i}} \frac{1}{r}. \quad (17)$$

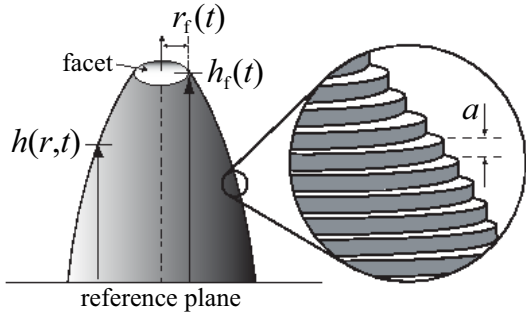


FIG. 1: Geometry of axisymmetric structure at macroscale (left) and microscale (right).

In view of Eq. (4), the i th-step chemical potential, μ_i , is proportional to the change of the total free energy, E_N , with respect to the step radius, r_i . By the formulas [7]

$$E_N = a \sum_i 2\pi r_i(t) [g_1 + g_3 V(r_i, r_{i+1})], \quad (18)$$

$$V(r_i, r_{i+1}) = \frac{1}{3} \frac{2r_{i+1}}{r_{i+1} + r_i} \left(\frac{a}{r_{i+1} - r_i} \right)^2, \quad (19)$$

$\mu_i = (\Omega/a)(2\pi r_i)^{-1}(\partial E_N/\partial r_i)$ is computed by

$$\mu_i(r, t) = \frac{\Omega g_1}{r_i} (1 + g\Phi_{i-1, i, i+1}), \quad (20)$$

where the (dimensionless) $\Phi_{i-1, i, i+1}$ couples three steps,

$$\Phi_{i-1, i, i+1} = \frac{\partial [r_i V(r_i, r_{i+1}) + r_{i-1} V(r_{i-1}, r_i)]}{\partial r_i}. \quad (21)$$

The use of Eq. (20) in Eq. (17) yields the adatom flux in terms of the step radii, $r_i(t)$.

It remains to express the i -th step velocity, $v_{st, i} = \dot{r}_i \equiv dr_i/dt$, in terms of the step radii, $r_i(t)$, for $t_n \leq t < t_{n+1}$ ($i \geq n+1$). By recourse to Eq. (5), we find that

$$\dot{r}_i = \frac{c_s D_s \Omega}{k_B T} \frac{1}{a r_i} \left(\frac{\mu_{i+1} - \mu_i}{\ln \frac{r_{i+1}}{r_i}} - \frac{\mu_i - \mu_{i-1}}{\ln \frac{r_i}{r_{i-1}}} \right) \quad (22)$$

where $i \geq n+3$. For $i = n+1$ and $n+2$, the step equations need to be modified, since each of these steps has one or no neighboring step on one side; in particular, for $i = n+1$ the second term of Eq. (22) disappears. We numerically solve ODEs (22) subject to the initial data

$$r_i(0) = r_0 + ia, \quad 1 \leq i \leq N. \quad (23)$$

C. Discrete boundary layer

Next, we provide an intuitive discussion on the notion of a discrete boundary layer based on step simulations. Our goal is to motivate the use of discontinuities for

certain continuum-scale variables across the facet edge (Sec. III E).

Figure 2 shows the step radii, $r_i(t)$, as a function of time, computed for $g = 0.1$ and $N = 10^3$; see also figures 2 and 4 in [4]. By inspection of the step trajectories, we observe that, in each time interval $t_n - \epsilon_n < t < t_n + \epsilon_n$ (where $0 < \epsilon_n < \min\{t_{n+1} - t_n, t_n - t_{n-1}\}$), the collapse of the n th (top) step causes a significant disturbance to the motion of *only very few* adjacent steps (numbered by i , $i \geq n+1$). This influence is manifested in the form of ripples in step motion, whose amplitudes rapidly decay with the radial distance from the topmost step. This picture also reveals a time scale separation: top steps (near the facet) move fast in comparison to the slow motion of steps away from the facet. In addition, the width of terraces away from the facet exhibits a relative slow spatial variation, at any given time. It is thus reasonable to describe the respective step density away from the facet via a continuum solution which can be informed about the behavior of top steps through suitable boundary conditions.

In each interval $t_n < t < t_{n+1}$, we empirically define the (time-dependent) discrete boundary layer as the narrow surface region near the facet edge formed by steps of index $i \geq n+1$ whose terrace width has rapid spatial and temporal variations. Evidently, this discrete layer contains a number of steps much smaller than the total number, N , of steps in the initial structure; the height of the boundary layer is of the order of a , the step size.

In the continuum limit, when terraces away from the facet are described by the continuous slope profile, we need to eliminate the above discrete layer, effectively replacing it by a (time-dependent) circle. We claim that, to a good approximation, this circle is the free boundary of the facet if the continuum chemical potential and its generating flux have appropriately defined jumps across this boundary. These jumps are phenomenologically described in Sec. III E.

D. Continuum scale: Reference case

We now describe the macroscopic free boundary problem in the reference case, which leaves out microstructure details. In Sec. V, we verify numerically that this approach is not consistent with step flow [9].

In our radial geometry, PDE (12) becomes

$$\frac{1}{B} \frac{\partial h}{\partial t} = \frac{1}{r^3} + g \frac{1}{r} \frac{\partial}{\partial r} r \frac{\partial}{\partial r} \frac{1}{r} \frac{\partial}{\partial r} (r m^2), \quad r > r_f(t), \quad (24)$$

where $m(r, t) = |\partial h(r, t)/\partial r|$, the positive surface slope. The differentiation of both sides of Eq. (12) with respect to r yields a PDE for m :

$$\frac{1}{B} \frac{\partial m}{\partial t} = \frac{3}{r^4} - g \frac{\partial}{\partial r} \frac{1}{r} \frac{\partial}{\partial r} r \frac{\partial}{\partial r} \frac{1}{r} \frac{\partial}{\partial r} (r m^2), \quad (25)$$

which is valid away from the facet.

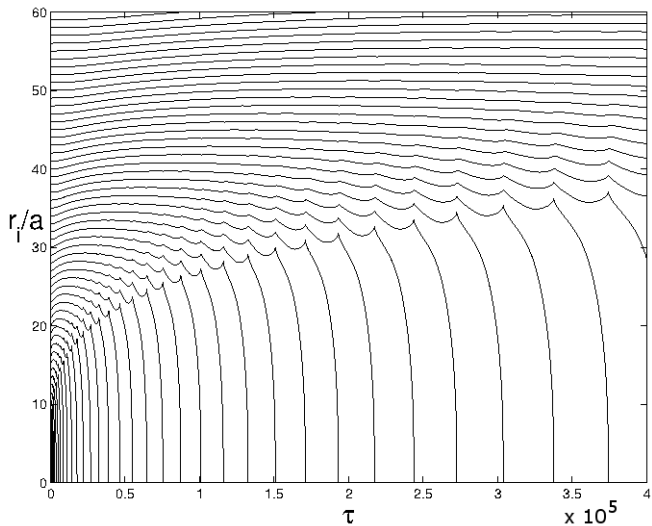


FIG. 2: Simulation data for step trajectories, $r_i(t)$, by numerically solving Eq. (22) with initial data (23), for $N = 10^3$, $r_0 = 0$ and $g = 0.1$. The non-dimensional time, τ , is defined by $\tau = [c_s D_s \Omega^2 a^{-4} g_1 / (k_B T)] t = (B a^{-4}) t$. The annihilations of top steps are evident.

Next, we outline the reference case for Eq. (25); see also [7]. By Eq. (11), the (radially directed) flux, ξ , generating the macroscale chemical potential outside the facet is

$$\xi(r, t) = \xi(r, t) \mathbf{e}_r, \quad \xi = 1 + gm^2, \quad r > r_f(t). \quad (26)$$

First, the continuity of slope yields

$$m(r_f(t), t) = 0; \quad (27)$$

in particular, $m(r, t) \approx \mathfrak{C}(t)[r - r_f(t)]^{1/2}$ near the facet, revealing the singular behavior of the continuum solution. Second, by continuity of height, $h(r_f(t)^+, t) = h_f(t)$, and Eq. (27) we obtain

$$\frac{r_f^3 \dot{h}_f}{B} = 1 - gr_f (\partial_r m^2 - 2r_f \partial_r^2 m^2 - r_f^2 \partial_r^3 m^2) \Big|_{r=r_f(t)^+}, \quad (28)$$

where $\partial_r \equiv \partial / \partial r$. Third, we address continuity of the radial adatom flux. By writing $\dot{h}_f + \Omega \nabla \cdot \mathfrak{J}_f = 0$ on the facet ($r < r_f$) and setting $\mathbf{e}_r \cdot \mathfrak{J}_f(r, t)$ equal to $\mathbf{e}_r \cdot \mathfrak{J}(r, t)$ at $r = r_f(t)$ we have

$$-\frac{r_f^3 \dot{h}_f}{2B} = 1 - gr_f (\partial_r m^2 + r_f \partial_r^2 m^2) \Big|_{r=r_f(t)^+}. \quad (29)$$

Fourth, by the continuous extension of the step chemical potential, we set $\mu(r_f^+, t)$ [cf. Eqs. (10) and (11)] equal to $\mu_f(r_f^-, t)$; the latter term stems from integration of the relation $\mathfrak{J}_f = -[c_s D_s / (k_B T)] \nabla \mu_f$ applied for $r < r_f$. Thus, we obtain

$$\frac{\Omega g_1}{4B} [r_f^3 \dot{h}_f + b(t)] = \Omega g_1 \left(\frac{1}{r} + g \partial_r m^2 \right) \Big|_{r=r_f(t)^+}. \quad (30)$$

A few comments on Eq. (30) are in order. The left-hand side is the chemical potential $\mu_f(r_f^-, t)$ on the facet [7], driven by changes of the facet height, where $b(t)$ is an integration constant; thus, this μ_f is directly influenced by the loss of top steps and can in principle incorporate discrete changes, if needed. The right-hand side of Eq. (30) is the continuum limit, $\mu(r_f^+, t)$, of the step chemical potential outside the facet, which expresses the variation of the step free energy according to Eq. (8).

In addition, in view of the relation $\mu = \Omega g_1 \nabla \cdot \xi$ on the entire surface, it is reasonable to continuously extend $\mathbf{e}_r \cdot \xi$ onto the facet, viz.,

$$\frac{1}{16B} [r_f^3 \dot{h}_f + 2r_f b(t)] = 1 + gm(r_f(t), t)^2 = 1, \quad (31)$$

where the left-hand side is the radial component of ξ on the facet. Boundary conditions (27)–(31) are supplemented by the requirement that

$$m(r, t) \rightarrow 1 \quad \text{as} \quad r \rightarrow \infty, \quad (32)$$

so that in the far field the slope is compatible with initial data (23). Equation (32) is meant to imply $\partial_r m \rightarrow 0$ as $r \rightarrow \infty$.

Equation (25) and conditions (27)–(32) are believed to form a meaningful free boundary problem. If the slope m is self similar, this problem is transformed accordingly and simplified (see Sec. V A for details).

Certain ingredients of this formulation are known to be questionable from a physical standpoint [1]. In particular, there is no compelling reason for μ and μ_f to be equal at the facet edge. In fact, since these chemical potentials express different physical mechanisms, μ and μ_f may be incompatible at the facet boundary. This observation suggests the scenario that Eq. (30) be replaced by a discontinuity condition (Sec. III E). In the same vein, there is no compelling reason for Eq. (31) to hold.

E. Continuum scale: Modified free boundary problem

In principle, the set of boundary conditions at the facet edge consistent with step flow should be derived from the continuum limit of ODEs (22). We have been unable to carry out this limit near the facet. Thus, we resort to speculation of the requisite boundary conditions, partly guided by results in [15] and numerical simulations. In particular, we modify Eqs. (30) and (31) to address the distinct origins of the two chemical potentials, defined in the regions away from and on the facet, by introducing jump discontinuities at the facet edge.

For later convenience, let

$$\mu_f(r, t) = \frac{\Omega g_1}{4B} [r^2 \dot{h}_f + b(t)], \quad r < r_f(t), \quad (33)$$

$$\xi_f(r, t) = \frac{1}{16B} [r^3 \dot{h}_f + 2rb(t)], \quad r < r_f(t). \quad (34)$$

We define the *global* large-scale chemical potential as

$$\mu_S(r, t) = \begin{cases} \mu(r, t) = \Omega g_1 r^{-1} \partial_r(r\xi), & r > r_f(t), \\ \mu_f(r, t), & r < r_f(t). \end{cases} \quad (35)$$

Accordingly, we define the generating flux

$$\xi_S(r, t) = \begin{cases} \xi(r, t) = 1 + gm^2, & r > r_f(t), \\ \xi_f(r, t), & r < r_f(t). \end{cases} \quad (36)$$

1. Jump conditions at facet edge

We require that the global large-scale chemical potential and its generating flux are discontinuous at the facet edge. As an extension of the formulation in [15], we express such discontinuities in terms of non-dimensional multiplicative factors, denoted $Q_\mu(t)$ and $Q_\xi(t)$. Accordingly, we formally impose

$$\mu_f(r_f(t)^-, t) = Q_\mu(t) \mu(r_f(t)^+, t), \quad (37)$$

$$\xi_f(r_f(t)^-, t) = Q_\xi(t) \xi(r_f(t)^+, t), \quad (38)$$

instead of applying Eqs. (30) and (31). Recall that $\mu(r_f^+, t) = \Omega g_1 [r_f^{-1} + g(\partial_r m^2)|_{r=r_f^+}]$ and $\xi(r_f^+, t) = 1$ are the limiting values of the continuum-scale chemical potential and its generating flux as r approaches the facet boundary from the smooth surface. The factors $Q_\mu(t)$ and $Q_\xi(t)$ in principle depend on the behavior of steps inside the discrete boundary layer. Note that setting $Q_\mu(t) \equiv 1 \equiv Q_\xi(t)$ corresponds to the reference case.

It can be claimed that Eq. (38) is a generalization of the shock-wave condition used for evaporation-condensation kinetics in [15]. It is tempting to compare Eq. (37) to the known Gibbs-Thomson formula, which describes the change in chemical potential or vapor pressure across an interface. Here, we are inclined to view the facet boundary as an interface separating two distinct phases: the facet, where individual step collapses occur, and the bulk of steps, which slowly evolves in a continuum-like fashion. In contrast to the Gibbs-Thomson relation, Eq. (37) allows for a jump $\mu_f(r_f(t)^-, t) - \mu(r_f(t)^+, t)$ that may depend on global features of the surface profile via μ in addition to the local characteristics (e.g., curvatures) of steps inside the discrete boundary layer.

Hence, the modified free boundary problem consists of PDE (25) under conditions (27)–(29), (32), (37) and (38). The remaining task is to provide formulas for Q_μ and Q_ξ .

2. Factors $Q_\mu(t)$ and $Q_\xi(t)$

In the spirit of [15], we seek conditions that incorporate the step collapses on top of the facet, taking into account steps that move inside the discrete boundary layer. We empirically construct jumps compatible with the following properties.

- (a) $Q_\ell(t)$ ($\ell = \mu, \xi$) is constant in every time interval $t_n < t < t_{n+1}$ for all $n = 0, 1, \dots$ ($t_0 = 0$).

- (b) $Q_\ell(t)$ is expressed in terms of curvatures (or radii) of a few top steps [cf. Eq. (15)]. In the simplest possible scenario, such a factor involves two consecutive steps and becomes unity if the step radii tend to coalesce, i.e., when $r_i \approx r_{i+1}$, and none of these steps collapses.

- (c) $Q_\xi(t) < 1$, by analogy with evaporation [15].

We first address the choice of Q_ξ . In the radial setting, a familiar geometric factor is $\mathcal{G}_i(t) = [r_{i+1}(t) + r_i(t)]/[2r_{i+1}(t)]$ [15], where $\mathcal{G}_i(t) < 1$ since we assume that the steps are ordered, $r_{i+1}(t) > r_i(t)$. Accordingly, by inspecting properties (a) and (b), we set

$$Q_\xi(t) = F(\mathcal{G}_n(t_n), \mathcal{G}_{n+1}(t_n), \dots, \mathcal{G}_{n+m-1}(t_n)) \quad (39)$$

for $t_n \leq t < t_{n+1}$; $\mathcal{G}_n(t_n) = 1/2$ by definition of t_n . Here, F is an multivariable function, to be discussed next.

We speculate the form of F , justifying our choice on the basis of our numerics later on (see Sec. V). In evaporation-condensation kinetics [15], the corresponding F depends on a single variable and is linear. In the present case, an analogously simple choice is

$$F = F(\mathcal{G}_n, \mathcal{G}_{n+1}) \equiv \frac{1}{2} [\mathcal{G}_n(t_n) + \mathcal{G}_{n+1}(t_n)], \quad (40)$$

a function of two variables, which expresses the arithmetic mean of the geometric factors $\mathcal{G}_n(t)$ and $\mathcal{G}_{n+1}(t)$ each evaluated at the step collapse times, $t = t_n$ ($n \geq 1$); thus, $Q_\xi(t) < 1$.

In Fig. 3, we show values of the piecewise constant $Q_\xi(t) = Q_\xi(t; g)$ in the intervals $t_n \leq t < t_{n+1}$ versus the step collapse number, n , for different values of the step interaction parameter, g . The data is obtained by numerically solving step ODEs (22) under Eq. (23). Evidently, for large t , $Q_\xi(t)$ asymptotically approaches a g -dependent constant. This behavior is consistent with the anticipated self-similar behavior of the discrete slopes, $m_i(t)$ (see Sec. V A).

Next, we turn our attention to the factor $Q_\mu(t)$. This type of jump has no counterpart in the case with evaporation, where the chemical potential is not invoked in the facet boundary conditions [15]. We find that the choice

$$Q_\mu(t) = F(\mathcal{G}_n, \mathcal{G}_{n+1})^{-1}, \quad t_n \leq t < t_{n+1}, \quad (41)$$

in combination with Eq. (39), produces results in excellent agreement with many-step simulations (see Sec. V).

Our choices of discontinuity factors are not unique. For example, another scenario includes having a discontinuous large-scale chemical potential in combination with a continuous generating flux (see Sec. VI A). In our efforts to implement this possibility, we had to make use of geometric factors evaluated at discrete times different from t_n . Our goal at this stage is to describe jump discontinuities that can form elements of a viable computational scheme. Thus, we choose to make use of the collapse times, t_n , in order to characterize the jumps. The *derivation* of the boundary conditions at the facet from the discrete scheme for steps remains an unresolved issue.

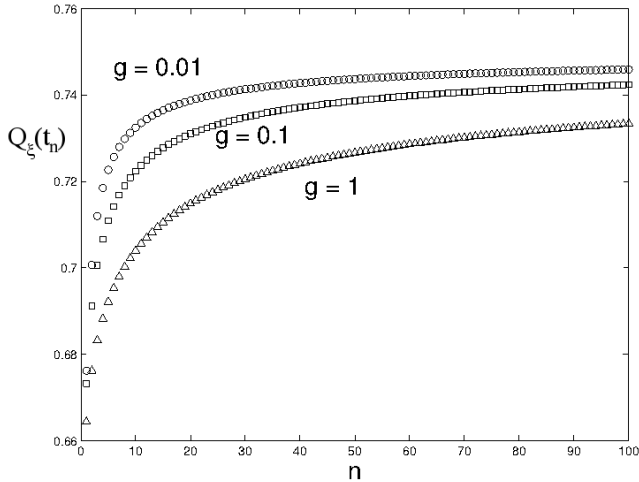


FIG. 3: Step simulation data for values of piecewise constant jump factor $Q_\xi(t) = Q_\xi(t; g)$ in intervals $t_n \leq t < t_{n+1}$ as a function of step collapse number, n . Circles: weak step interaction, $g = 0.01$; squares: $g = 0.1$; and triangles: $g = 1$.

IV. HYBRID DISCRETE-CONTINUUM SCHEME

In this section, we formulate a computational scheme that couples the continuum theory with the motion of only a few steps near the facet, in an effort to validate the modified free boundary problem introduced in Sec. III E. The numerical results from this scheme are in excellent agreement with many-step simulations (see Sec. V).

Two important features of the jumps Q_μ and Q_ξ of Sec. III E are: (i) the jumps approach a g -dependent constant for $n \gg 1$ (after many steps collapse); and (ii) the jumps depend only on a small number of steps. These features rely on the assumed step kinetics and energetics, e.g. the property that each step interacts only with its nearest neighbors. For example, in the hypothetical scenario with long-range step-step interactions, plausible jump factors may depend on many step positions.

The use of Q_μ and Q_ξ aims to incorporate into the continuum model the fast motion of steps inside the discrete boundary layer (see Fig. 2). In this sense, the proposed hybrid scheme links the slow motion of steps away from the facet, where continuum theory is applicable, to rapidly changing (due to step annihilations) step trajectories near the facet.

In our scheme, we start with the self-similar continuum solution of the reference case, which does not require any input from steps (Sec. III D). As the time advances and the number of step annihilations increases, we successively improve this solution through solving a few ODEs for steps inside the discrete boundary layer in combination with the modified free boundary problem of Sec. III E. In solving a few ODEs, say, for $M = 3$ steps, we have to provide a reasonable approximation for the

radii of adjacent steps interacting with these M steps. For this purpose, we use

$$r_{i+1} \approx r_i + \frac{a}{m(r_i, t)}. \quad (42)$$

Here, $m(r, t)$ denotes a continuum-scale solution for the surface slope; by our self-similarity ansatz, $m(r, t) \approx \mathfrak{M}(\eta)$ where $\eta = r/(Bt)^{1/4}$ (see Sec. V A).

Our iterative scheme consists of the following stages.

1. Compute $m(r, t)$ in the self-similar regime, i.e., via $\mathfrak{M}(\eta)$, for the reference case (Sec. III D).
2. Simulate M top steps ($3 \leq M \ll N$) in the time interval $\tilde{t}_{n_\diamond} < t \leq \tilde{t}_{n_*}$. The M step ODEs are terminated by use of Eq. (42) where $i = n + M + l$, $n_\diamond \leq n < n_*$, and $l = 0, 1$. The number of simulated steps is M at all times; when the i -th step collapses, i.e., r_i becomes 0, the respective ODE is removed and the ODE for r_{i+M} is added to the system. Here, \tilde{t}_n denotes the n -th step collapse time computed within this scheme. This part is initiated for $n_\diamond = 0$ and $n_* \geq 1$ with $\tilde{t}_0 = 0$.
3. Re-compute the self-similar slope $\mathfrak{M}(\eta)$ by using the jump boundary conditions (Sec. III E) at $t = \tilde{t}_{n_*}$, where Q_ξ and Q_μ are determined by Eqs. (39)–(41) from the previously resolved, reduced system of M steps.
4. Iterate: Repeat parts 2 and 3 by replacement of n_\diamond by the previous n_* and enforcement of one step collapse (advancing n_* to $n_\diamond + 2$). Continue, advancing t until many steps have collapsed.

Our hybrid scheme is heuristic. The total number of iterations, $\mathcal{N}(g)$, in principle decreases with the step-step interaction parameter, g (see Sec. V B). However, it has not been possible to a priori predict how many iterations are needed precisely, and thus how many times the jump conditions must be applied, until satisfactory accuracy is achieved. This would require a systematic error analysis of our scheme, which is not pursued here.

V. NUMERICAL RESULTS

In this section, we provide details of our numerical simulations for the relaxation of an initial cone. Specifically, we carry out computations by our hybrid scheme and compare the results to many-step simulations.

A. Self-similarity

Our step simulations for conical initial data indicate that the discrete slope, $m_i = a/(r_{i+1} - r_i)$, becomes self-similar at long time, as is also observed in [4, 9]. In this section, we outline consequences of this behavior.

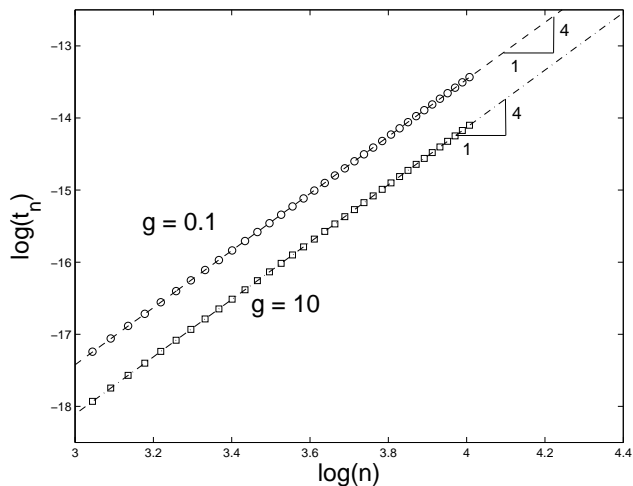


FIG. 4: Log-log plot of collapse times t_n versus n , for step interaction parameters $g = 0.1$ and $g = 10$.

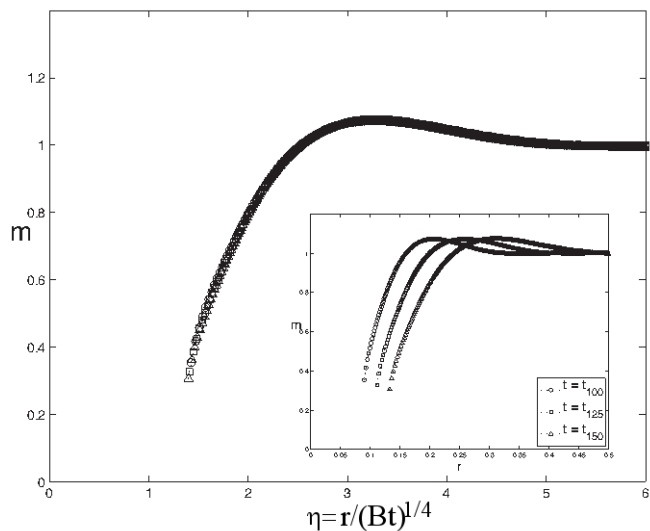


FIG. 5: Discrete slope m_i versus: radial coordinate r_i for different times $t = t_n$ (inset); and scaled variable $r_i/(Bt_n)^{1/4}$ (main plot). The step-step interaction parameter equals $g = 0.1$ and the number of collapsing steps is $n = 100, 125, 150$.

In particular, we hypothesize that evolution PDE (25) reduces to a similarity ODE in the context of the free boundary problems of Sec. III. At the moment, we are not aware of any analytical proof for the existence of such self-similar continuum solution.

An indication of self similarity is the asymptotic behavior $t_n \approx t_*(g)n^4$ for $n \gg 1$; cf. Fig. 4. In addition, the plots of $m_i(t; g)$ versus r_i for any fixed step annihilation time, $t = t_n$, approximately yield a single (g -dependent) curve if r_i is scaled by $(Bt)^{1/4}$ and $n \gg 1$; cf. Fig. 5.

Following [9], we assume that $m(r, t) \approx \mathfrak{M}(\eta)$ where $\eta = r/(Bt)^{1/4}$ and t is large enough. Thus, PDE (25) is

converted to the similarity ODE [9]

$$-\frac{\eta}{4} \frac{d\mathfrak{M}}{d\eta} = \frac{3}{\eta^4} - g \frac{d}{d\eta} \frac{1}{\eta} \frac{d}{d\eta} \eta \frac{d}{d\eta} \frac{1}{\eta} \frac{d}{d\eta} (\eta \mathfrak{M}^2), \quad (43)$$

for $\eta > \eta_f \equiv r_f/(Bt)^{1/4}$, outside the facet.

The requisite boundary conditions are transformed accordingly. The reference case is presented in [9]. For the modified boundary value problem, conditions (27)–(29), (37), and (38) at the facet edge become

$$\mathfrak{M}(\eta_f) = 0, \quad (44)$$

$$-\kappa \eta_f^3 = 1 + g \eta_f \left[-(\mathfrak{M}^2)' + 2\eta_f (\mathfrak{M}^2)'' + \eta_f^2 (\mathfrak{M}^2)''' \right] \Big|_{\eta=\eta_f}, \quad (45)$$

$$\frac{1}{2} \kappa \eta_f^3 = 1 - g \eta_f \left[(\mathfrak{M}^2)' + \eta_f (\mathfrak{M}^2)'' \right] \Big|_{\eta=\eta_f}, \quad (46)$$

$$\frac{1}{8} \kappa \eta_f^3 = 2\mathcal{Q}_\xi - \mathcal{Q}_\mu \left[1 + g \eta_f (\mathfrak{M}^2)' \Big|_{\eta=\eta_f} \right], \quad (47)$$

where $\mathcal{Q}_\mu = \lim_{n \rightarrow \infty} \mathcal{Q}_\mu(t_n)$ and $\mathcal{Q}_\xi = \lim_{n \rightarrow \infty} \mathcal{Q}_\xi(t_n)$. Equation (47) accounts for both the conditions on μ and ξ , Eqs. (37) and (38), where the related constant of integration, $b(t)$, was eliminated. In the above, $\kappa = -\dot{h}_f(Bt)^{3/4}/B$ and the prime denotes differentiation with respect to the self-similarity variable, η . In addition, by far-field condition (32), we have

$$\mathfrak{M}(\eta) \rightarrow 1 \quad \text{as } \eta \rightarrow \infty. \quad (48)$$

We use $m(r, t) \approx \mathfrak{M}(\eta)$ at all stages of our hybrid scheme (Sec. IV). Since the scheme starts from $t = 0$ with a self-similar solution, which in principle holds at long time, we expect significant numerical error in the surface slope computed at small times.

We numerically compute the self-similar solution $\mathfrak{M}(\eta)$ by applying the Matlab boundary value problem solver `bvp4c` to ODE (43) for different values of the interaction parameter g . The main plots in Figs. 6 and 7 show outcomes of step simulations for the discrete slope and the continuum-scale slope computed via the jump conditions; the corresponding factors \mathcal{Q}_μ and \mathcal{Q}_ξ are evaluated via the full system of step ODEs (22). Evidently, the jump conditions yield results in excellent agreement with step simulations when the discrete simulation data is used for the jump factors. In contrast, the insets in Figs. 6 and 7 confirm that the reference case is in principle not consistent with step simulations.

B. Results of hybrid scheme

We now implement our hybrid scheme (Sec. IV) for different values of the interaction parameter, g . For this purpose, we simulate a small number of steps, $M = 3$, which is minimal within the discrete model of nearest-neighbor step-step interactions. The main conclusion

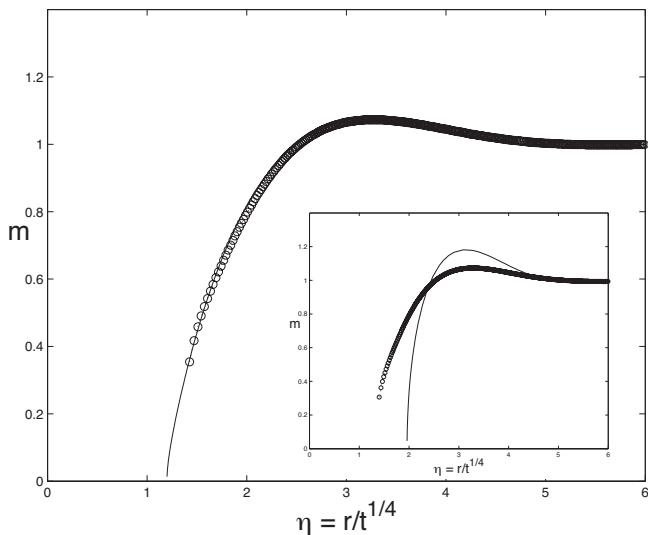


FIG. 6: Comparison of discrete slope (circles) versus continuum slope (solid curve) using: (i) natural boundary conditions (inset), and (ii) jump boundary conditions (main plot) when $g = 0.1$. The time unit is chosen so that $B = 1$.

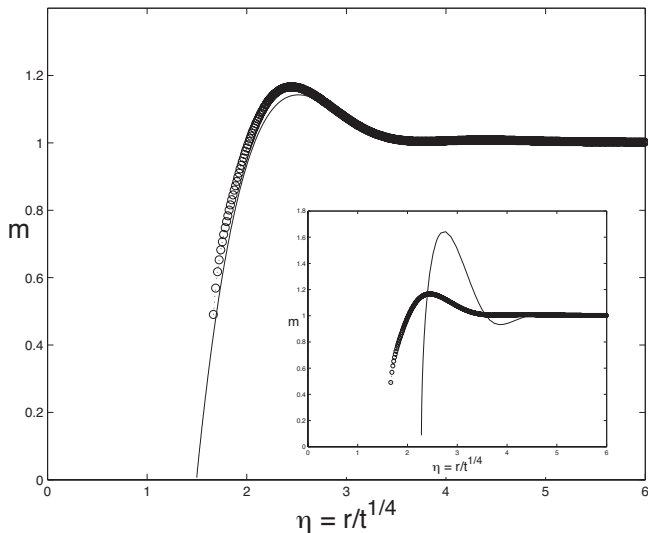


FIG. 7: Comparison of discrete slope (circles) versus continuum slope (solid curve) using: (i) natural boundary conditions (inset), and (ii) jump boundary conditions (main plot) when $g = 0.01$. The time unit is chosen so that $B = 1$.

drawn from our numerical results is that the self-similar continuum slope, produced by the slope of the reference case after a sufficient number of iterations of the hybrid scheme, approaches the discrete slope computed by the many-step simulations. This apparent convergence of our scheme is illustrated for three different values of g in Fig. 8.

We observe that the number of iterations, \mathcal{N} , decreases with the step interaction parameter, g . This behavior is expected, stemming from the property that increasing g

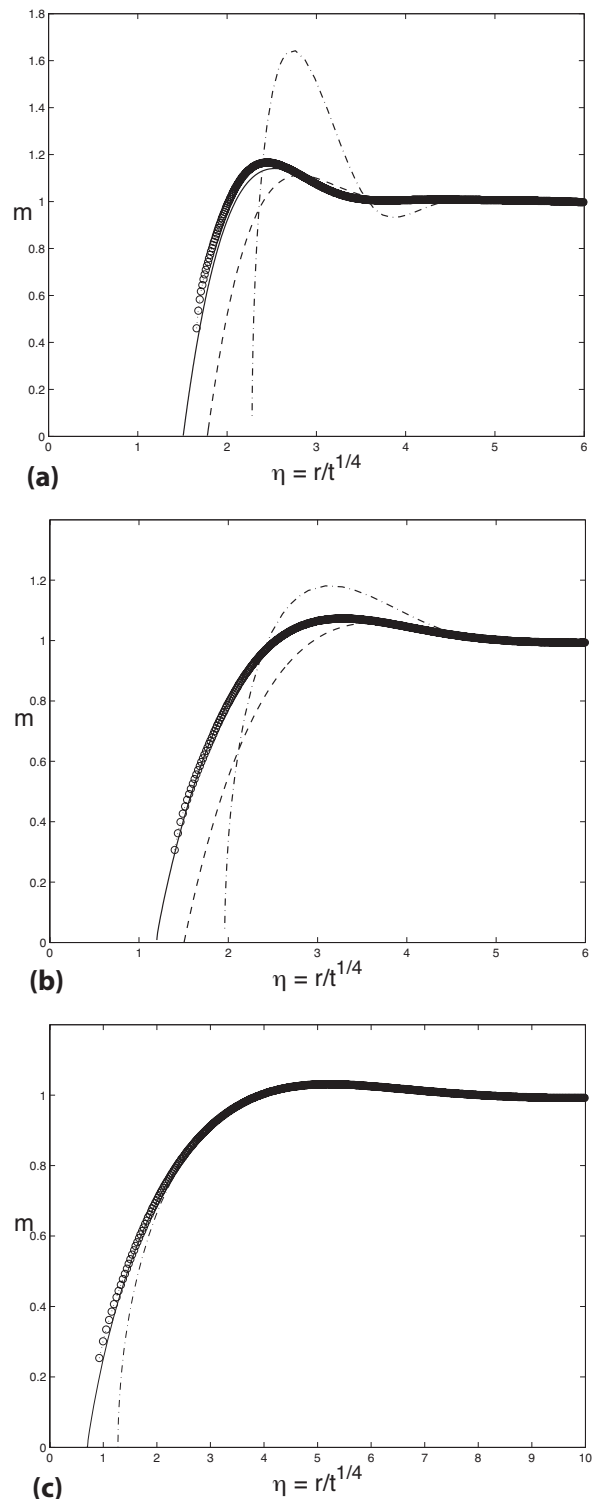


FIG. 8: Comparison of discrete slope (circles) from step simulations and continuum self-similar solution by hybrid scheme for $M = 3$, $n_\infty = 0$ and $n_* = 4$. The reference case (dash-dots) is the starting continuum solution. The hybrid scheme sufficiently approaches a continuum slope (solid curve) after \mathcal{N} iterations. An intermediate solution (dashes) is produced by a smaller number of iterations, \mathcal{N}_1 . (a) $g = 0.01$, with $\mathcal{N} = 66$ and $\mathcal{N}_1 = 6$. (b) $g = 0.1$, with $\mathcal{N} = 16$ and $\mathcal{N}_1 = 1$. (c) $g = 1$, with $\mathcal{N} = 1$. The time unit is chosen so that $B = 1$.

causes a lower step density near the facet edge as strongly interacting steps tend to be farther apart. In fact, the facet (at fixed time t) shrinks while the jump factors Q_μ and Q_ξ approach unity as g increases, which suppresses discrete effects and the need for a truly hybrid scheme. In contrast, small values of g result in an increase of the number of iterations, \mathcal{N} , because the weakly interacting steps tend to form a bunch near the facet edge.

VI. DISCUSSION

In this section, we discuss plausible modifications of our formulation. In particular, we address a free boundary problem where a *single jump* is introduced. We also comment on the use of an alternate hybrid scheme in which the step ODEs are linked to the continuum theory via the step-drop condition [9]. Finally, we discuss open challenges in 2D.

A. Boundary conditions with single jump

It is compelling to ask whether the jump factors of Eqs. (39)-(41) can be chosen uniquely. We claim that, in the context of our empirical approach, the answer to this question is negative if the jump factors are evaluated at times different from the step collapse times, t_n .

For example, let us consider the scenario where continuum equation (43) is solved numerically by imposition of only *one* jump condition. Specifically, suppose we choose to apply *either* the jump (Q_μ) in the chemical potential *or* the jump (Q_ξ) in the flux generating the chemical potential. Then, by our numerical computations the ensuing continuum theory predicts surface slopes *not* consistent with step motion *if* the jump is evaluated at the step collapse times, t_n . This observation indicates that the sequence of times at which a single jump should be evaluated may not be a priori characterized; the sequence consists of adjustable parameters whose linkage to $r_i(t)$ appears as unknown, and needs to be determined. This hypothetical formulation is deemed as impractical for viable computations of facet evolution. In contrast, the step collapse times t_n are characterized by $r_n(t_n) = 0$, which can be incorporated into a hybrid scheme.

Following this scenario of a single jump, our numerics also yield the sequence of times, \hat{t}_n , required to achieve agreement of continuum predictions with step simulations; $t_n < \hat{t}_n < t_{n+1}$. Each \hat{t}_n is close to t_n for sufficiently large values of g .

B. Step-drop condition: Alternate hybrid scheme

It of some interest to examine whether a viable hybrid scheme can be devised on the basis of step-drop condition (14) [9]. Although we have not yet reached a definitive conclusion in this direction, numerical results sug-

gest that our “jump formulation” of boundary conditions (Sec. III E), relying on discontinuities of two thermodynamic variables, forms a more viable approach.

First, we comment on a comparison of the two formulations. Evidently, the jump formulation maintains the thermodynamic structure of continuum theory, since it retains variables such as the chemical potential which is the variational derivative of the surface free energy outside the facet. On the other hand, the step-drop condition makes direct use of the vertical facet speed which is remotely connected to the thermodynamic structure. In view of these features, we believe that the jump formulation bears certain advantages over the step-drop condition. For example, computations of the surface slope based on the former are more robust.

We made an attempt to construct a hybrid scheme that iteratively utilizes the step-drop condition. Numerical results of this scheme indicate poor convergence after a large number of iterations, in contrast to the outcomes of the hybrid scheme in Sec. IV. This behavior is possibly due to significant numerical error in the continuum solution because of error in the step collapse time differences, $t_{n+1} - t_n$, explicitly used in the step drop condition.

C. Issues with facets in 2D

The extension of our formulation to full 2D, e.g., for periodic surface corrugations, calls for improvements of our approach. An emerging issue is to numerically solve the full PDE for the surface height, abandoning the assumption of self similarity for the positive surface slope. The resolution of this issue is the subject of work in progress for the radial setting. A plausible numerical treatment is offered by the finite element method, which has been a valuable tool in studies of surface morphological evolution, e.g., in [37]. However, commonly known versions of this method correspond to the reference case. The incorporation of jump conditions across the facet boundary into this method is an open problem.

A related issue is the nature of the jumps at the edges of 2D, non-circular facets. In the radial setting, the jump factors, Q_μ and Q_ξ , depend on the radii of top steps. In a more general 2D setting, a plausible scenario is to use Eq. (39) by replacing r_i in each $\mathcal{G}_i(t)$ by the Lagrangian coordinate of step motion invoked in [34]. In this context, it is of course necessary to formulate the respective equations of motion for steps by use of these Lagrangian coordinates. This task is left for near-future work.

VII. CONCLUSION

Motivated by the need to predict non-equilibrium properties of crystals, we revisited a classic problem in crystal surface morphological evolution: the formulation of a continuum theory for evolving facets. Our perspective is different from previous approaches, as we aim to

reconcile the discrete nature of step motion with a continuum description without using any adjustable parameters. For an axisymmetric, semi-infinite structure with a single facet, we showed that in the self-similar regime, at sufficiently long time: (i) a PDE for the surface slope outside the facet can account for the facet microstructure through certain step-driven jump discontinuities at the facet for a continuum-scale chemical potential and the flux that generates it; and (ii) this theory can be implemented efficiently by an iterative two-scale, hybrid scheme which couples the PDE away from the facet with the motion of only three top steps lying inside a discrete boundary layer near the facet.

Our approach indicates the special role of the surface chemical potential in formulating a *minimal* continuum model consistent with step flow for the near-equilibrium evolution of crystal facets. The facet boundary is treated as an interface separating two phases: the bulk of steps whose motion is described through variations of the surface free energy and a Fick-type law of diffusion; and the facet whose height decrease is dictated by individual step collapses. The jump imposed on the continuum chemical potential depends both on the (local) curvatures of steps near the facet and the global surface profile. Physically, a jump condition may be expected, since the chemical potential on the facet, driven by the loss of individual steps, is distinct from the chemical potential away the facet, driven by variations of the surface free energy. Mathematically, it is tempting to claim that the imposition of such discontinuities is consistent with recent interpretations of the facet as a shock-type wave [15, 38]; however,

we have been unable to place this statement on firm analytical grounds.

Our treatment reveals the nature of the singular behavior of the surface slope at the facet edge. This behavior is due to the reduction of the discrete boundary layer to the sharp facet boundary; then, requisite details of step flow are no longer transparent. Our work indicates how such details can possibly be retained through jump discontinuities within a continuum framework.

While numerical outcomes of the hybrid scheme warrant attention to our approach, there remain key unresolved questions. The jumps introduced here are speculative; a rigorous analysis would be desirable. We have only treated the radial geometry and diffusion-limited kinetics. Nevertheless, we are optimistic that our free boundary treatment utilizing jump boundary conditions can be extended to other systems with facets. Specifically, the attachment-detachment limited regime in radial geometry should be a tractable case. An analogous hybrid approach to the full (2+1)-dimensional setting is an open problem. In the same vein, the PDE for the height profile must be solved numerically without assuming a self-similar $|\nabla h|$. We hope that our present contribution will stimulate further research in this direction.

ACKNOWLEDGMENTS

The authors wish to thank Professor R. V. Kohn, Professor R. H. Nochetto, and Professor J. D. Weeks for valuable discussions. This work was supported by the NSF via Grant No. DMS 08-47587.

-
- [1] W. Selke and P. M. Duxbury, Phys. Rev. B **52**, 17468 (1995).
- [2] A. Chame, S. Rousset, H. P. Bonzel, and J. Villain, Bulgarian Chem. Commun. **29**, 398 (1996/97).
- [3] N. Israeli and D. Kandel, Phys. Rev. Lett. **80**, 3300 (1998).
- [4] N. Israeli and D. Kandel, Phys. Rev. B **60**, 5946 (1999).
- [5] H. Spohn, J. Phys. I (France) **3**, 69 (1993).
- [6] E. E. Gruber and W. W. Mullins, J. Phys. Chem. Solids. **28**, 875 (1967).
- [7] D. Margetis, M. J. Aziz, and H. A. Stone, Phys. Rev. B **71**, 165432 (2005).
- [8] N. Israeli and D. Kandel, Phys. Rev. Lett. **88**, 116103 (2002).
- [9] D. Margetis, P.-W. Fok, M. J. Aziz, and H. A. Stone, Phys. Rev. Lett. **97**, 096102 (2006).
- [10] H. P. Bonzel, E. Preuss, and B. Steffen, Appl. Phys. A **35**, 1 (1984).
- [11] H. P. Bonzel and E. Preuss, Surf. Sci. **336**, 209 (1995).
- [12] V. B. Shenoy and L. B. Freund, J. Mech. Phys. Solids **50**, 1817 (2002).
- [13] N. Israeli and D. Kandel, Phys. Rev. B **62**, 13707 (2000).
- [14] N. Israeli, H.-C. Jeong, D. Kandel, and J. D. Weeks, Phys. Rev. B **61**, 5698 (2000).
- [15] K. Nakamura and D. Margetis, Multiscale Model. Simul. **11**, 244 (2013).
- [16] A. Rettori and J. Villain, J. Phys. (France) **49**, 257 (1988).
- [17] F. Lançon and J. Villain, in *Kinetics of Ordering and Growth at Surfaces*, edited by M. Lagally (Plenum, New York, 1990).
- [18] M. Ozdemir and A. Zangwill, Phys. Rev. B **42**, 5013 (1990).
- [19] E. B. Tadmor, M. Ortiz, and R. Phillips, Phil. Mag. A **73**, 1529 (1996).
- [20] W. E and B. Engquist, Comm. Math. Sci. **1**, 87 (2003).
- [21] W. L. Briggs, V. E. Henson, and S. F. McCormick, *A Multigrid Tutorial* (Society for Industrial and Applied Mathematics, Philadelphia, PA, 2000).
- [22] N. G. Hadjikonstantinou, J. Comput. Phys. **154**, 245 (1999).
- [23] W. Kossel, Nachrichten von der Gesellschaft der Wissenschaften zu Göttingen: Math. Phys. (Göttingen: Royal Society of Sciences and Humanities, 1927), p. 135.
- [24] I. N. Stranski, Z. Chem. **136**, 259 (1928).
- [25] W. K. Burton, N. Cabrera, and F. C. Frank, Philos. Trans. R. Soc. London Ser. A **243**, 299 (1951).
- [26] A. Pimpinelli and J. Villain, *Physics of Crystal Growth* (Cambridge University Press, Cambridge, UK, 1999).
- [27] H.-C. Jeong and E. D. Williams, Surf. Sci. Rep. **34**, 171

- (1999).
- [28] V. I. Marchenko and A. Ya. Parshin, *Sov. Phys. JETP* **52**, 129 (1980).
- [29] C. Jayaprakash, C. Rottman, and W. F. Saam, *Phys. Rev. B* **30**, 6549 (1984).
- [30] W. W. Mullins, in *Metal Surfaces*, American Society of Metals, edited by W. D. Robertson and N. A. Gjostein (ASM, Metals Park, OH, 1962), pp. 17–66.
- [31] A. A. Chernov and E. D. Dukova, *Kristallografiya* **5**, 627 (1960).
- [32] G. Ehrlich and F. Hudda, *J. Chem. Phys.* **44**, 1039 (1966); R. L. Schwoebel and E. J. Shipsey, *J. Appl. Phys.* **37**, 3682 (1966).
- [33] P. Nozières, *J. Phys. (France)* **48**, 1605 (1987).
- [34] D. Margetis and R. V. Kohn, *Multiscale Model. Simul.* **5**, 729 (2006).
- [35] R. Kobayashi and Y. Giga, *J. Stat. Phys.* **95**, 1187 (1999).
- [36] Y. Kashima, *Adv. Math. Sci. Appl.* **14**, 49 (2004).
- [37] A. Bonito, R. H. Nochetto, J. Quah, and D. Margetis, *Phys. Rev. E* **79**, 050601(R) (2009).
- [38] P.-W. Fok, R. R. Rosales, and D. Margetis, *Phys. Rev. B* **78**, 235401 (2008).